Open access • Journal Article • DOI:10.1063/1.1708177

Influence of Jog Concentration on the Conservative Motion of Dislocations in Copper — Source link

Pierre Petroff, Jack Washburn

Published on: 01 Dec 1966 - Journal of Applied Physics (American Institute of Physics)

Topics: Critical resolved shear stress and Dislocation

Title
INFLUENCE OF JOG CONCENTRATION ON THE CONSERVATIVE MOTION OF DISLOCATIONS IN COPPER

Authors
Petroff, Pierre
Washburn, Jack.

Publication Date
1966-05-01

UCRL-16859

University of California

Ernest O. Lawrence Radiation Laboratory

INFLUENCE OF JOG CONCENTRATION ON THE CONSERVATIVE MOTION OF DISLOCATIONS IN COPPER

DISCLAIMER

Journal of Applied Physics

UCRL-16859
Preprint

UNIVERSITY OF CALIFORNIA

Lawrence Radiation Laboratory
Berkeley, California

AEC Contract No. W-7405-eng-48

INFLUENCE OF JOG CONCENTRATION ON THE CONSERVATIVE MOTION OF DISLOCATIONS IN COPPER

Pierre Petroff and Jack Washburn

May 1966

INFLUENCE OF JOG CONCENTRATION ON THE CONSERVATIVE MOTION OF DISLOCATIONS IN COPPER

Pierre Petroff and Jack Washburn

Inorganic Materials Research Division, Lawrence Radiation Laboratory, and Department of Mineral Technology, College of Engineering, University of California, Berkeley, California

May 1966

ABSTRACT

In an annealed crystal of low dislocation density the critical resolved shear stress necessary to move circular prismatic edge dislocation loops along their glide cylinders was compared to the range of stresses within which various segments of the three dimensional network began to move. Etch-pit observations showed that the first segments of the network moved at $2g/mm^2$ but that only 60% had moved when the maximum resolved shear stress had reached $38g/mm^2$.

Circular prismatic loops, which because of their shape have a high jog concentration, were found to move at a critical resolved shear stress greater than $50g/mm^2$. It was suggested that jog concentration should be expected to vary from one segment to another of the three dimensional network in an annealed crystal and that this is probably one important reason for the widely different stresses at which individual segments begin to move.

INFLUENCE OF JOG CONCENTRATION ON THE CONSERVATIVE MOTION OF DISLOCATIONS IN COPPER

Pierre Petroff and Jack Washburn

Inorganic Materials Research Division, Lawrence Radiation Laboratory
Department of Mineral Technology, College of Engineering
University of California, Berkeley, California

May 1966

INTRODUCTION

It has been shown by dislocation etch pit experiments[1] and by sensitive stress-strain measurements[2] that loading an annealed copper crystal to 4 g/mm^2 resolved shear stress on the $\langle 110 \rangle$ $\{111\}$ systems is sufficient to cause plastic deformation. The plastic component of the strain increases slowly with increasing applied stress up to the yield stress. In an initially highly perfect crystal the density of dislocations can increase several orders of magnitude during this pre-yield plastic deformation.

It is not yet clear exactly what factors control the stress at which yielding or rapid multiplication of strain begins. One possibility is that slip bands, within which most of the plastic strain is concentrated after the yield, cannot develop until a stress level is reached at which dislocation segments not lying on or very near $\{111\}$ can move. Therefore it is of interest to try to measure the critical stress for conservative motion of dislocation segments containing high jog concentrations.

The etch pit observations suggest that some dislocation segments are much less mobile than others. Even after application of a stress an order of magnitude greater than that at which the first dislocations move, there are still dislocations that have not moved.

The purpose of the present experiments was to compare the critical stress for motion of heavily jogged edge dislocations with the range of critical stress found for the dislocation segments that make up the three dimensional dislocation network in an annealed crystal.

EXPERIMENTAL PROCEDURE

Copper single crystals of 1 inch diameter and 3 inches length and a $\langle 111 \rangle$ axis were grown by the Czochralski method from 99.999% copper. From these crystals, parallelepipeds of about (5mm x 5mm x 25mm) were cut by acid sawing, two opposite (5mm x 25mm) faces were made parallel to {111}. The samples were then polished on a chemical polishing lathe with a solution of (50% HNO_3, 25% H_3PO_4, 25% acetic acid) - so that the {111} faces were parallel within 2 degrees, to the crystallographic plane. During this operation the specimens were thinned down to a thickness of 0.5mm. All the specimens were then annealed under purified helium at 1075°C for 100 hours. This resulted in a decrease in dislocation density from 10^5 per cm^2 to about 2×10^4 dislocations per cm^2 as determined from etch pit counts.

To measure the critical stress for motion of dislocations of the three dimensional network these crystals were stressed as cantilever beams as shown in Fig. 1. A known weight was applied by means of a quartz knife which was placed on one arm of an analytical balance.

After annealing and before deformation the crystals were electropolished at 50°C in a solution of 33% HNO_3, 67% Methanol and placed in stainless steel grips. They were etched in a solution of 1 part bromine, 15 parts glacial acetic acid, 25 parts hydrochloric acid, 90 parts water for 5 to 7 seconds.[3] After deformation the crystals were re-etched for 3 seconds and rinsed in ethyl alcohol. Dislocations that had moved appeared as flat bottomed pits of triangular shape. Smaller pits corresponded to moved dislocations or to new dislocations and the sharp large pits to unmoved dislocations (see Figs. 2 and 3).

The handling of the specimens during mounting and etching was done in a way to avoid any extraneous deformation. Prior to etching the specimen was set in the grips and the different operations of etching and rinsing were done with the specimen in the grips. The weight of the specimens was approximately 0.20g. Therefore the shear stresses that resulted from its own weight were less by an order of magnitude than those due to the loading. The errors in measuring the dimensions of the specimen and the applied load corresponded to an uncertainty in the resolved shear stress of about 4%.

The mobility of heavily jogged edge dislocations was studied by producing prismatic half loops and observing their spacing in an inverse pile up. Half loops were produced by dropping alumina balls of 30μ to 40μ in diameter on the surface of the sample from a height of 20cm. On impact they caused a deformation of the crystal similar to that due to differential volume changes around precipitates during cooling as it was observed by Barnes and Mazey in quenched Cu.[4] After impacting, the samples were etched for 7 seconds. Figure 4 shows the type of deformation surrounding the point of impact: rows of prismatic loops form a "rosette" which has branches extending along <110> directions.

RESULTS AND DISCUSSIONS

A. Motion of Grown-in Dislocations

From classical mechanics the stress produced by the cantilever loading is given in the elastic region by $\tau = \frac{6PL}{a^2b}$ where a,b,c, are the dimensions of the specimen as defined in Fig. 1 - P is the applied load and L is the distance from the point of application of the load. If the top surface of the specimen is taken as $(1\bar{1}1)$ and the maximum tensile stress is along $[\bar{1}12]$ then the resolved shear stresses had values

$\tau_m = 0.408\tau$ for $(11\bar{1})$, $[011]$ and (111) $[10\bar{1}]$ slip systems

$\tau_R = 0.272\tau$ for $(\bar{1}11)$, $[0\bar{1}1]$ and $(\bar{1}11)$ $[\bar{1}01]$ slip systems

$(11\bar{1})$ $[\bar{1}10]$ slip system

(111) $[\bar{1}10]$ slip system

$\tau_R = 0.135\tau$ for (111) $[0\bar{1}1]$ and $(11\bar{1})$, $[\bar{1}01]$ slip systems

The percentage N of moved dislocations was observed along the length of 3 samples by counting the number of flat bottomed pits N_1 per cm^2 and the number of sharp bottomed pits N_2 per cm^2. By extrapolation of the curve obtained by plotting $N = \frac{100N_1}{N_1+N_2}$ as a function of the maximum resolved shear stress τ_m corresponding to different positions along the specimen, the critical stress required to displace the most mobile dislocation was found to be $2.5 g/mm^2$.

This is even lower than the $4 g/mm^2$ obtained by Young[1] but is about the same as the stress at which plastic strain was first detected by Tinder.[2] Unforturately the meaning of this critical stress is not entirely clear because the first dislocations to move may have been those that could shorten their length by the motion. Therefore the applied stress may have been supplying only a part of the driving force. It is also impossible in this experiment to know to which slip system a given dislocation belongs. However, few dislocations were found to have moved along the trace of the plane of minimum resolved shear stress at right angles to the direction of the maximum tensile stress. It was assumed that the dislocations that moved along a given trace had the Burgers vector resulting in the highest resolved shear stress for that plane. It was also assumed that the dislocations that moved lay approximately on {111} planes. For a resolved shear stress τ_m=38g/mm^2 still only 40% of the dislocations had moved. Because only one of the six Burgers vectors lies at right angles to the direction of maximum tension this relatively small fraction of moved dislocations suggests that many dislocation segments are far less mobile than is suggested by the critical stress of 2.5g/mm^2.

By matching old flat pits with new small pits the distance moved by dislocations was also observed as a function of the applied resolved shear stress (see Figs. 2 and 3). The measurements were made by careful scanning of the pictures using a grid of lines parallel to the two principal slip directions. The largest distances of motion were assumed to correspond to dislocations which had moved in the slip system of highest resolved shear stress. The displacements of at least three dislocations were used for each point of the curve of Fig. 6. Extrapolation of this curve to zero displacement also gave a value of 2g/mm^2 for the critical stress required to move the most mobile dislocations. The average displacement of a dislocation for τ_m = 5g/mm^2 was about 10^{-3} cm.

B. Motion of Prismatic Half Loops

In an inverse pile up of loops such as those that extend outward from the point of impact in Fig. 4 the forward-most loop is pushed outward along its glide cylinder by its elastic interaction with the other loops on the same glide cylinder.

Newman and Bullough[5] considered the interaction of a number of prismatic circular loops on the same glide cylinder. The shear stress on the glide cylinder τ, due to a single loop of radius a was evaluated as:

$$\tau = \frac{\alpha bG}{4\pi(1-\nu)a}$$

where B = Bergers vector of the loop

α = Dimensionless parameter which was a function of the loop radius, a (see Fig. 7)

ν = Poisson's ratio

G = Shear modulus

The shear stress on the glide cylinder due to a single loop decreases rapidly with the distance Z from the loop. When the ratio $\frac{Z}{2a}$ is > 2.5 the shear stress can be approximated by:

$$\tau = \frac{3ba^3G}{(1-\nu)Z^4}$$

The shear stress τ^* acting on the last loop of a row of five loops will be $\tau^* = \sum_{i=1}^{4} \tau_i\ (a_i Z_i)$. Where τ_i is the shear stress exerted by the ith loop of the row on the last loop of the row. Therefore, by measuring the distance between it and the other loops it is possible to estimate the critical stress necessary to cause it to glide. It should stop moving when the stress due to the other loops is just equal to the frictional stress resisting its motion. In these experiments we are dealing with half loops at an external surface.

It will be assumed that the shear stress on the glide cylinder due to a half loop is the same as for a complete prismatic loop: for a prismatic loop several microns in diameter shear stresses are zero at all points of the plane of symmetry that cuts through the loop and contains the Burgers vector. Although the normal stresses are not zero across this plane it will be assumed as an approximation that no major change occurs in the magnitude of the shear stresses if the crystal is cut into two parts along this plane. For the calculations we have considered only rows of more than five loops, these loops being well aligned along a <110> direction and regularly spaced as shown in Fig. 4. It was thought that these were cases where there had not been strong interactions with parts of the grown-in network.

The average measured distances between the last loop and the next three loops were

$$Z_1 = 5.93\ 10^{-4}\text{cm.}$$
$$Z_2 = 10.25\ 10^{-4}\text{cm.}$$
$$Z_3 = 14.66\ 10^{-4}\text{cm.}$$

The average radius for the loops was: $2.18\ 10^{-4}$cm.

Taking α from Fig. 7 and with $G = 4.95\text{x}10^6$ g/mm^2, $\tau^* = 56.7$ g/mm.

This relatively high stress necessary for conservative motion of prismatic loops which, because of the shape of the impacting particles, almost certainly had a semicircular shape, probably explains the results of part (A). Many of those dislocations that did not move at an applied stress of 38 g/mm^2 may have had relatively high jog concentrations. The concentration of jogs or steps where a line passes from one high density {111} layer to the next should vary for different dislocation segments in an annealed crystal. At high temperature the dislocation network has approached a configuration of metastable equilibrium by both conservative and nonconservative motions. Assuming that the energy associated with a jog is small, elastic strain energy is minimized when dislocation segments approach linearity and nodes become symmetrical.

Therefore in metals of medium to high stacking fault energy few segments should be expected to lie exactly on low index glide planes. Recent direct observations by Merlini et. al.[6] are consistent with this picture.

CONCLUSIONS

1. At room temperature the grown in dislocations in an annealed 99.999% copper single crystal with an initial dislocation density of 2×10^4 per cm^2 start to move at a critical shear stress of about $2g/mm^2$. However, even after the applied stress has been raised to $38g/mm^2$, only 40% of the dislocations have moved.

2. Punched prismatic dislocation loops in the same copper specimens move along their glide cylinders at a critical shear stress, $\tau^* \simeq 56g/mm^2$.

3. The greatly different mobility of different segments of the annealed network of dislocations is probably due to differences in their jog concentration.

ACKNOWLEDGEMENTS

This work was done under the auspices of the United States Atomic Energy Commission.

REFERENCES

1. F. W. Young, J. Appl. Phys. 32, 1815 (1961).
2. R. Tinder and J. Washburn, Acta Met. 12, 129 (1964).
3. J. D. Livingston, J. Appl. Phys. 31, 1071 (1960).
4. R. S. Barnes and D. J. Mazey, Acta Met. 11, 281 (1963).
5. R. C. Newmann and R. Bullough, Phil Mag., 921 (1960).
6. Alfonso E. Merlini, F. A. Sherrill, and Fred W. Young Jr., Bull. Am Phys. Soc. 10, 324 (1965).

FIGURE CAPTIONS

Fig. 1 Specimen mount for handling and cantilever beam loading.

Fig. 2 Typical field of view showing dislocation positions before and after application of a load. The direction of maximum tensile stress was parallel to [$\bar{1}$12] and the initial and final position of moved dislocations are indicated by arrows. (x 610)

Fig. 3 Motion of dislocations: Dislocation A moved to A' during first loading. Dislocation B which appeared after first test moved to B' after second loading. The direction of maximum tensile stress was parallel to [$\bar{1}$12]. (x 3800)

Fig. 4 Rosette of dislocation loops produced by impact of a 30 micron alumina sphere. (x 2750)

Fig. 5 Percent of moved dislocations vs maximum resolved shear stress.

Fig. 6 Average distance moved vs maximum resolved shear stress.

Fig. 7 Dimensionless parameter α (from Newman and Bullough[3]) used for calculation of resolved shear stress acting on the glide cylinder of a prismatic loop.

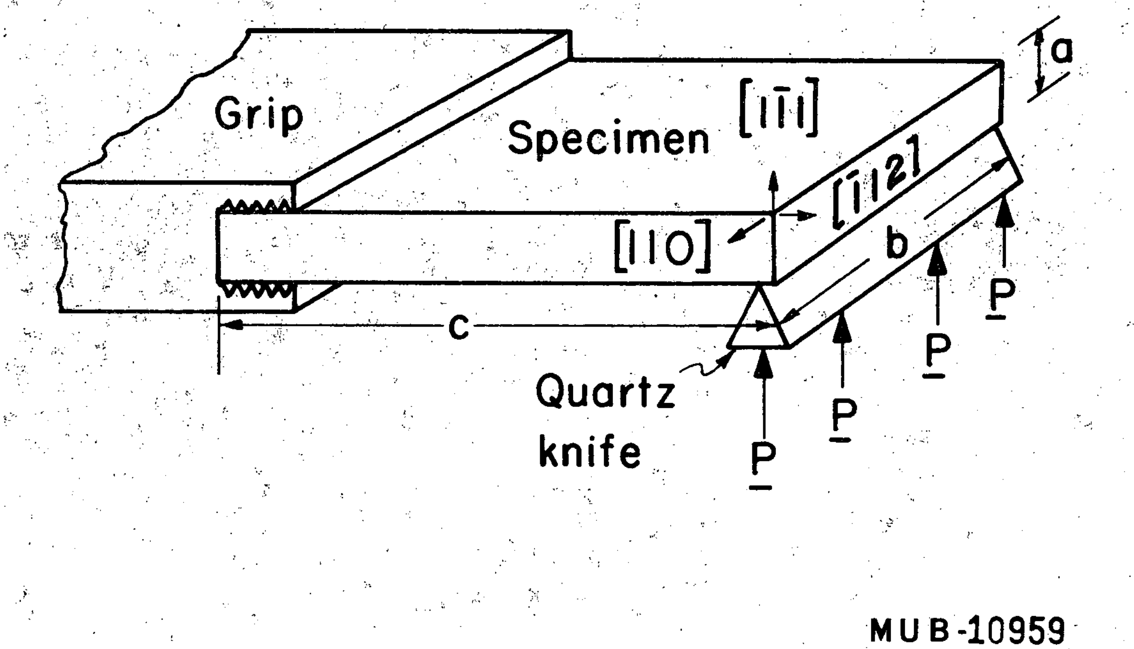
Grip
Specimen
[1$\bar{1}$1]
[$\bar{1}$12]
[110]
a
b
c
Quartz knife
P
P
P
P
MUB-10959

Fig. 1

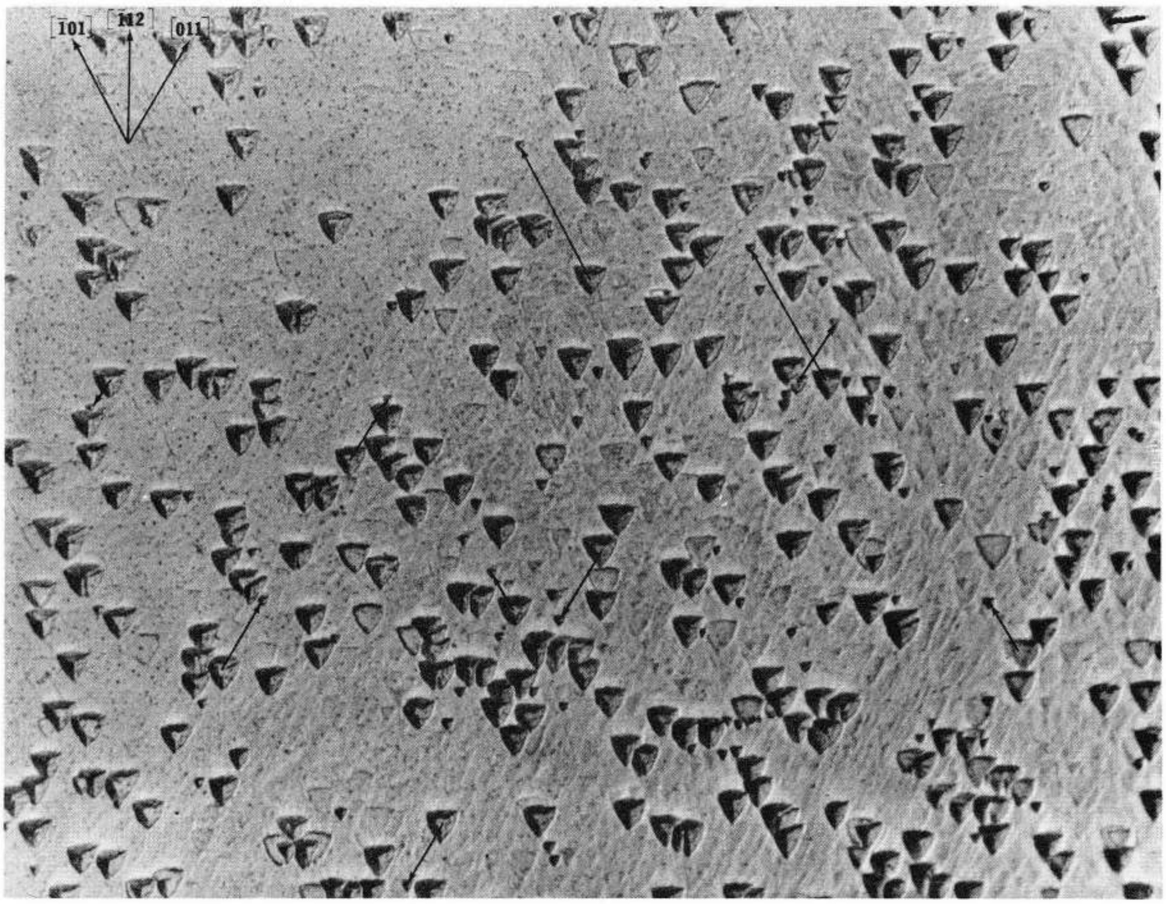

ZN-5670

Fig. 2

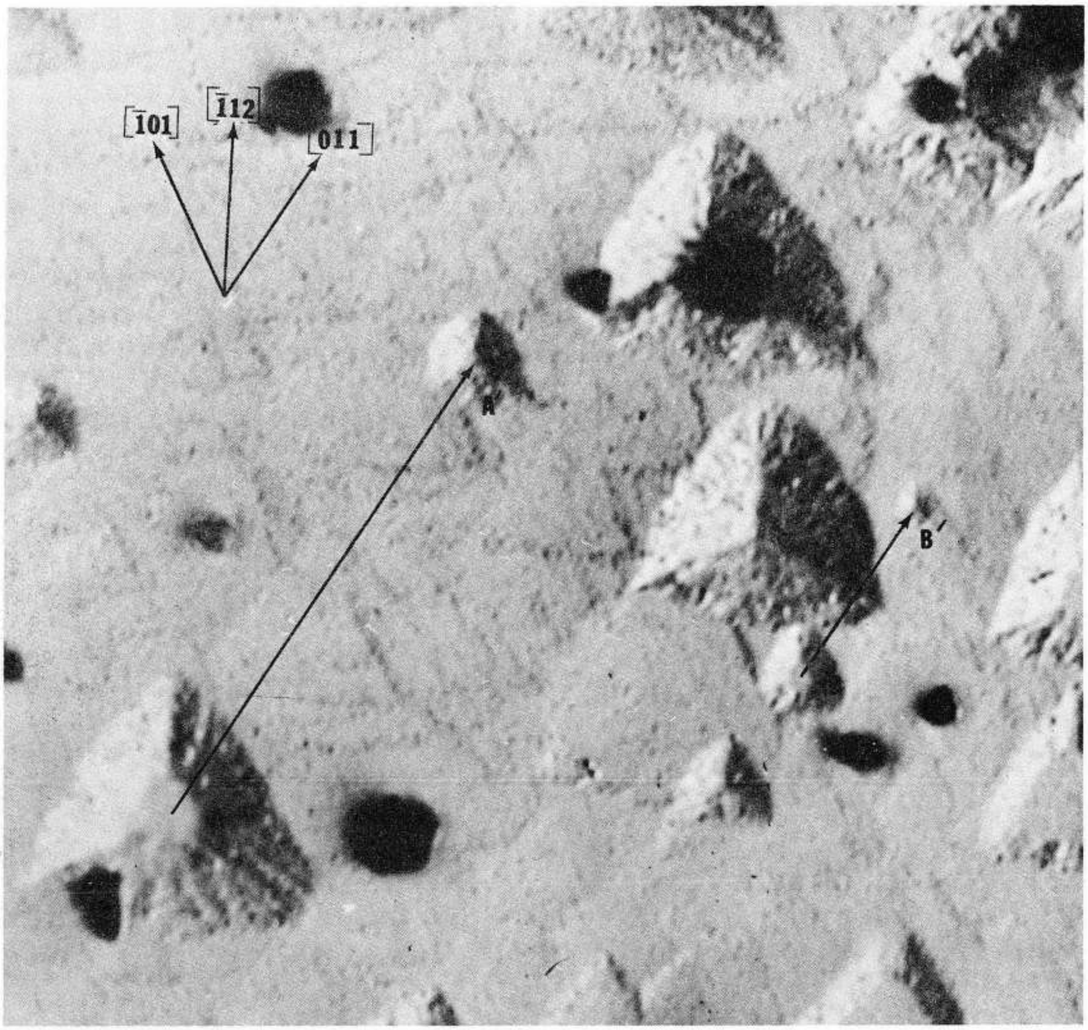

ZN-5671

Fig. 3

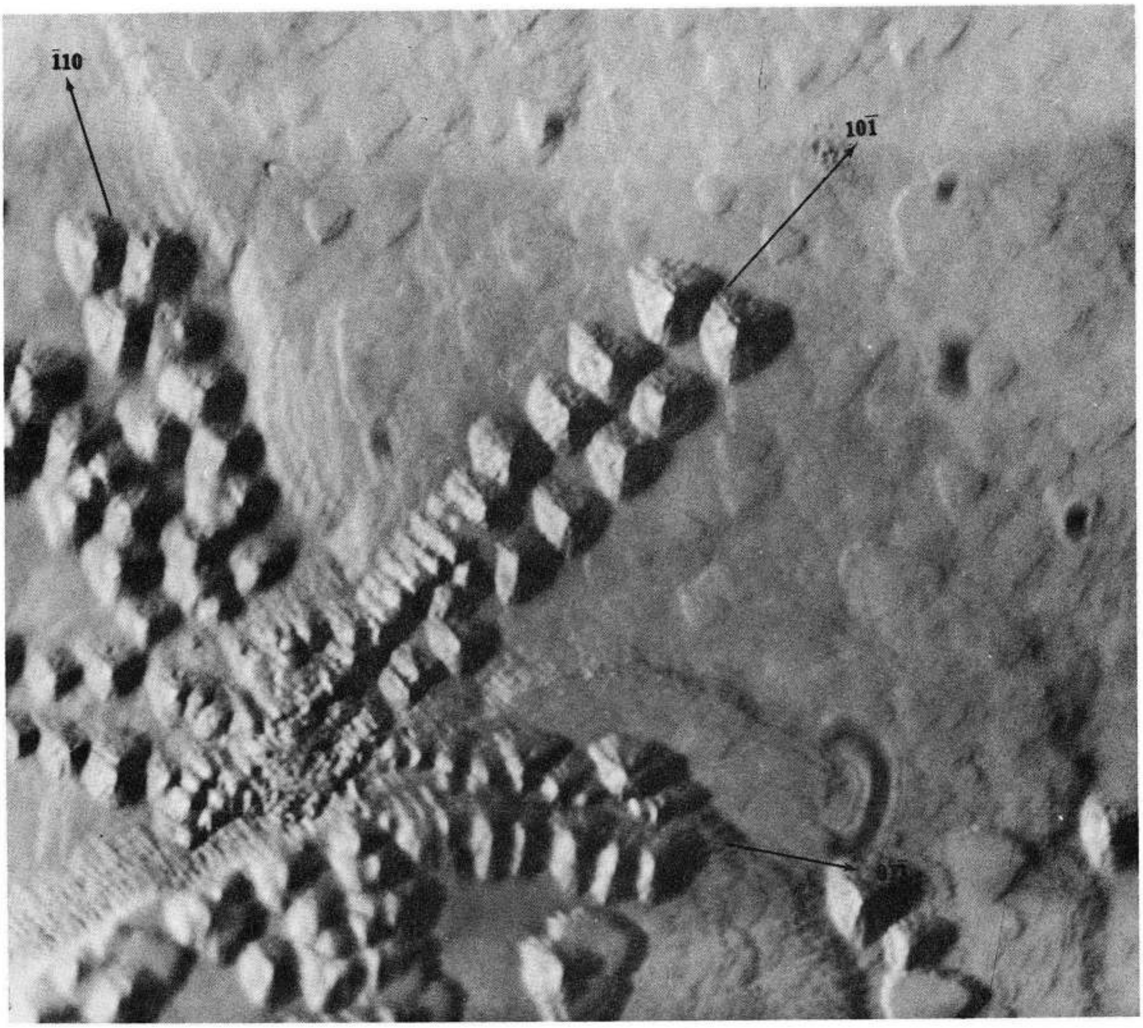

ZN-5672

Fig. 4

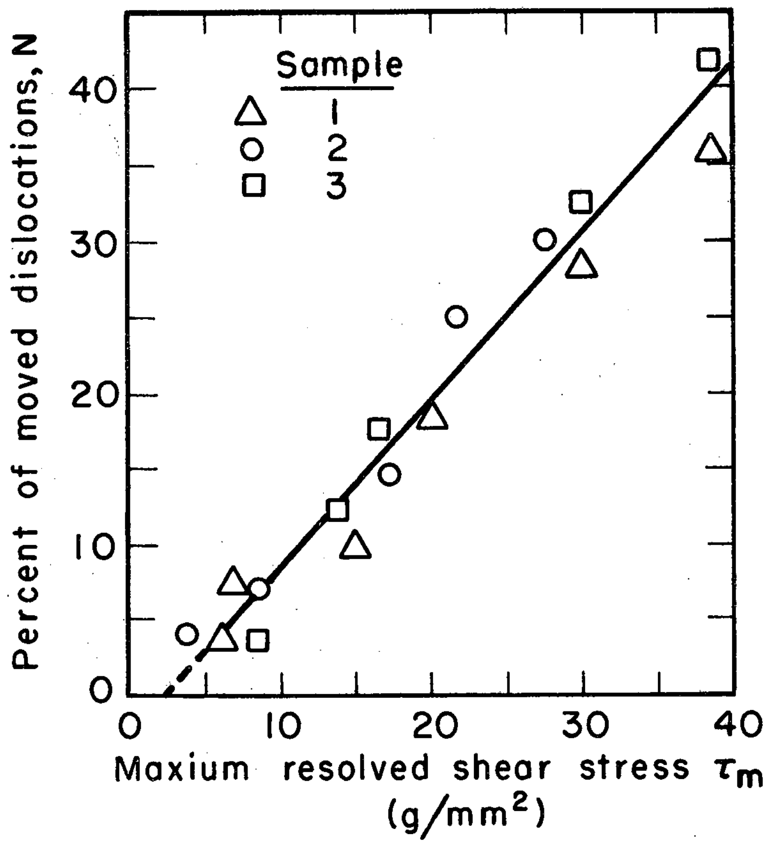

MUB-10958

Fig. 5

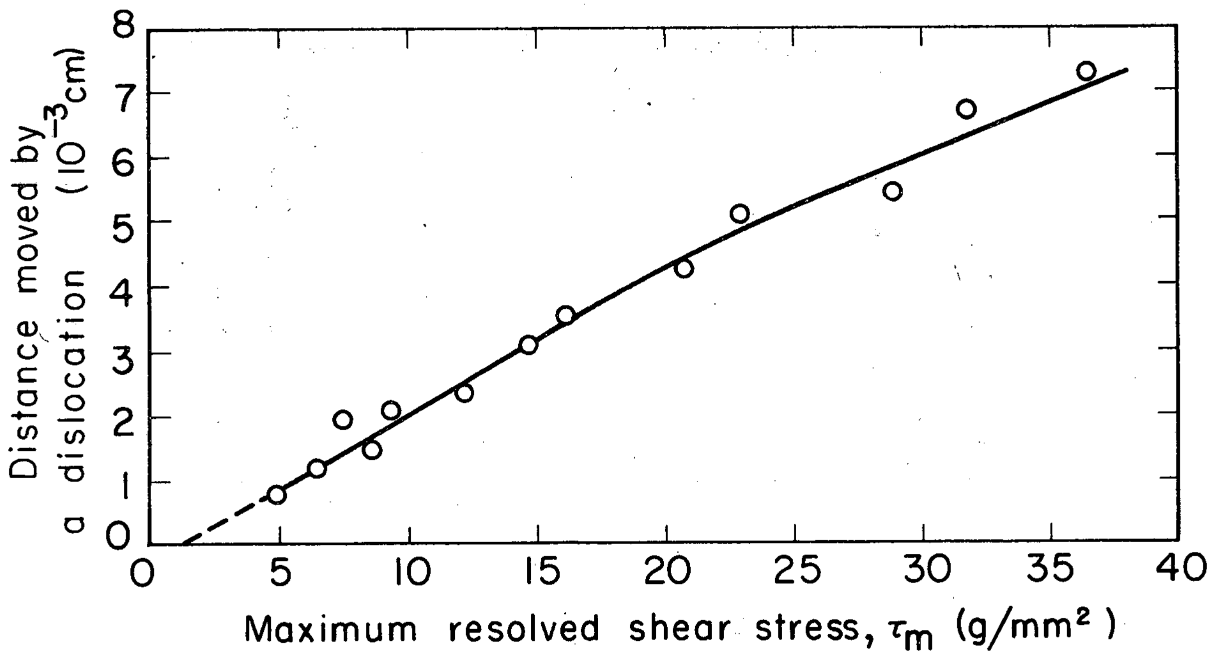

MUB-10960

Fig. 6

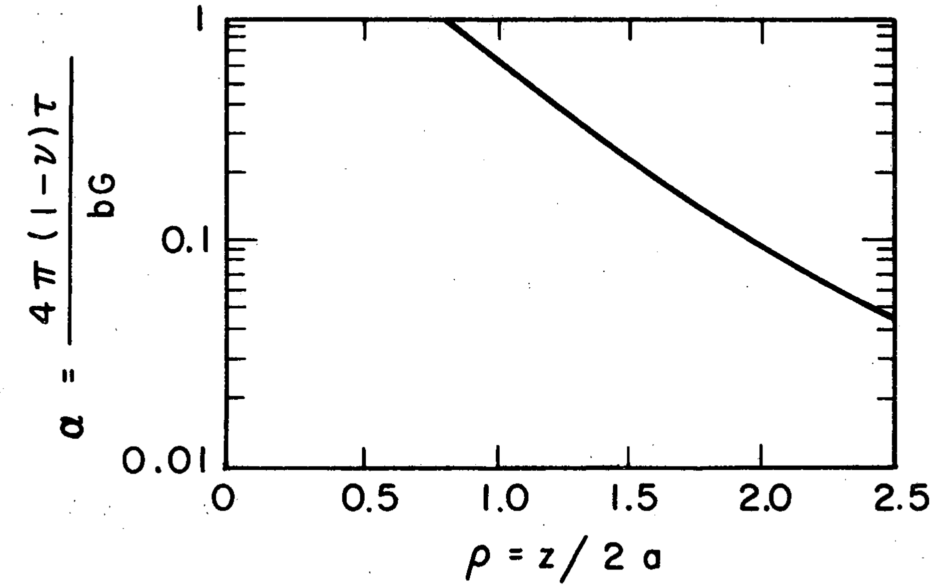

MUB-10957

Fig. 7